Mon. Not. R. Astron. Soc. **000**, 000–000 (0000) Printed 25 May 2015 (MN LATEX style file v2.2)

Searching for nova shells around cataclysmic variables

D. I. Sahman,[1⋆] V. S. Dhillon,[1] C. Knigge,[2] T. R. Marsh[3]
[1] *Department of Physics and Astronomy, University of Sheffield, Sheffield S3 7RH, UK*
[2] *School of Physics & Astronomy, University of Southampton, Southampton SO17 1BJ, UK*
[3] *Department of Physics, University of Warwick, Coventry CV4 7AL, UK*

arXiv:1505.06048v1 [astro-ph.HE] 22 May 2015

Accepted 2015 May 16. Received 2015 April 17

ABSTRACT

We present the results of a search for nova shells around 101 cataclysmic variables (CVs), using Hα images taken with the 4.2-m William Herschel Telescope (WHT) and the 2.5-m Isaac Newton Telescope Photometric Hα Survey of the Northern Galactic Plane (IPHAS). Both telescopes are located on La Palma. We concentrated our WHT search on nova-like variables, whilst our IPHAS search covered all CVs in the IPHAS footprint. We found one shell out of the 24 nova-like variables we examined. The newly discovered shell is around V1315 Aql and has a radius of $\sim 2.5'$, indicative of a nova eruption approximately 120 years ago. This result is consistent with the idea that the high mass-transfer rate exhibited by nova-like variables is due to enhanced irradiation of the secondary by the hot white dwarf following a recent nova eruption. The implications of our observations for the lifetime of the nova-like variable phase are discussed.

We also examined 4 asynchronous polars, but found no new shells around any of them, so we are unable to confirm that a recent nova eruption is the cause of the asynchronicity in the white dwarf spin. We find tentative evidence of a faint shell around the dwarf nova V1363 Cyg. In addition, we find evidence for a light echo around the nova V2275 Cyg, which erupted in 2001, indicative of an earlier nova eruption ~ 300 years ago, making V2275 Cyg a possible recurrent nova.

Key words: stars: novae, cataclysmic variables.

1 INTRODUCTION

Cataclysmic variables (CVs) are close binary systems in which a white dwarf (WD) accretes material from a secondary star, via Roche-lobe overflow (see Warner 1995 for a review). CVs are classified observationally into 3 main sub-types – the novae, the dwarf novae and the nova-like variables. The *novae* are defined as systems in which only a single nova eruption has been observed. Nova eruptions have typical amplitudes of 10 magnitudes and are believed to be due to the thermonuclear runaway of hydrogen-rich material accreted onto the surface of the white dwarf. The *dwarf novae* (DNe) are defined as systems which undergo quasi-regular (on timescales of weeks-months) outbursts of much smaller amplitude (typically 6 magnitudes). Dwarf nova outbursts are believed to be due to instabilities in the accretion disc causing the sudden collapse of large quantities of material onto the white dwarf. The *nova-like* variables (NLs) are the non-eruptive CVs, i.e. objects which have never been observed to show nova or dwarf nova outbursts. The absence of dwarf nova outbursts in NLs is believed to be due to their high mass-transfer rates, producing ionised accretion discs in which the disc-instability mechanism that causes outbursts is suppressed (Osaki 1974). The mass transfer rates in NLs are $\dot{M} \sim 10^{-8} - 10^{-9}$ M$_\odot$ yr^{-1} whereas DNe have rates of $\dot{M} \sim 10^{-10} - 10^{-11}$ M$_\odot$ yr^{-1}. Note that throughout this paper, when we refer to NLs we mean non-magnetic systems, i.e. we do not include in our definition systems that accrete via magnetic field lines, such as polars and intermediate polars.

Our understanding of CV evolution has made great strides in recent years (e.g. see Knigge et al. 2011, Knigge 2011). For example, there is now strong evidence that the 2–3 hr period gap in the orbital period distribution of CVs is indeed due to disrupted angular momentum loss (Patterson et al. 2005), the first "period-bounce" CVs, in which the secondary star has lost so much mass to the WD that it falls below the hydrogen–burning limit, have now been discovered (Littlefair et al. 2008), and the predicted spike of

⋆ E-mail: d.sahman@sheffield.ac.uk; vik.dhillon@sheffield.ac.uk

© 0000 RAS

systems at the period minimum has been revealed (Gänsicke et al. 2009).

One of the remaining unsolved problems in CV evolution is: how can the different types of CV co-exist at the same orbital period? Theory predicts that all CVs evolve from longer to shorter orbital periods on timescales of gigayears, and as they do so the mass-transfer rate also declines (e.g. see Fig. 19 of Knigge et al. 2011). At periods longer than approximately 5 hrs, all CVs should have high mass-transfer rates and appear as NLs, whereas below this period the lower mass-transfer rate allows the disc-instability mechanism to operate and all CVs should appear as DNe. This theoretical expectation, however, is in stark contrast to observations, which show that the fraction of nova-like variables to dwarf novae is actually highest at 3 hr periods and then declines to longer periods (e.g. see Fig. 18 of Knigge et al. 2011).

It is possible that CVs cycle between NL and DN states on timescales shorter than the gigayear evolutionary timescale of the binary, thereby explaining the co-existence of NLs and DNe at the same orbital period. Two mechanisms for such a cycle have been proposed. Both mechanisms invoke cyclical variation in the irradiation of the secondary, which in turn drives cyclical variation of $\dot{M}$ with timescales of the order of $\sim 10^4 - 10^7$ yrs.

The first idea is that there is an irradiation feedback mechanism. The flux from the WD illuminates the inner face of the secondary which flattens the temperature gradient in the photosphere, leading to an expansion in the radius of the secondary and an increase in $\dot{M}$ above the secular mean (see Büning & Ritter 2004 and references therein). The enhanced $\dot{M}$ drives an increase in the radius of the secondary's Roche lobe. Eventually the expansion of the secondary star cannot keep pace with the Roche lobe expansion, leading to a lower $\dot{M}$, and hence a reduction in the irradiating flux. Consequently, the secondary begins to shrink and the feedback mechanism operates in reverse as the mass transfer rate reduces. Büning & Ritter (2004) found that this mechanism could produce limit cycles in $\dot{M}$ of the appropriate timescales (see Fig. 5 of Knigge et al. 2011), causing CVs to cycle between DN and NL states. However, their models show that systems just above the period gap are actually stable and do not undergo cycles. Hence, although this model explains why some NLs and DNe may co-exist at the same orbital period, it does not explain why the irradiation-driven feedback mechanism would make the NL fraction highest around 3 hr and decline towards longer periods.

The second hypothesis for variable $\dot{M}$ is a nova-induced cycle. Some fraction of the energy released in the nova event will heat up the WD, leading to increased irradiation and subsequent bloating of the secondary. Following the nova event, the system would have a high $\dot{M}$ and appear as a NL. As the WD cools, the radius of the secondary would return to its secular value, and hence $\dot{M}$ will reduce and the system changes to a DN. In this model, therefore, CVs are expected to cycle between nova, NL and DN states, on timescales of $10^4 - 10^5$ yrs (see Shara et al. 1986), thereby explaining the co-existence of these CV sub-types at the same orbital period. Like the irradiation feedback mechanism, however, this nova cycle model does not explain why the NL fraction is highest around 3 hr and declines towards longer periods.

The cyclical evolution of CVs through nova, NL and DN phases recently received observational support from the discovery that BK Lyn appears to have evolved through all three phases since its likely nova outburst in the year AD 101 (Patterson et al. 2013). A second piece of evidence has come from the discovery of nova shells around the dwarf novae Z Cam and AT Cnc (Shara et al. 2007, Shara et al. 2012), verifying that they must have passed through an earlier nova phase. A more obvious place than DNe to find nova shells is actually around NLs, as the nova-induced cycle theory suggests that the high $\dot{M}$ in NLs could be due to a recent nova eruption. Finding shells around the highest accretion–rate NLs would lend further support to the existence of nova-induced cycles and hence help explain why systems with different $\dot{M}$ are found at the same orbital period.

In this paper we present the results of an Hα imaging survey of the fields surrounding a sample of 101 cataclysmic variables, 24 of them NLs, with the aim of identifying nova shells around the central binary.

2 OBSERVATIONS AND DATA REDUCTION

2.1 William Herschel Telescope

2.1.1 Search strategy

The choices of telescope aperture and field of view for this project were dictated by the expected brightness and radii of the nova shells around CVs. Recombination theory tells us that the Hα luminosity per unit volume of a nova shell is proportional to density squared, and hence the total luminosity of the shell is inversely proportional to volume. If we assume that the shell expands at a constant velocity, then its volume increases as the cube of time. Therefore, the luminosity is inversely proportional to time cubed, and the surface brightness decreases as time to the fifth power. This expectation has been empirically confirmed by Downes et al. (2001) who found that the Hα surface brightness of nova shells diminishes as $t^{-4.8}$, although novae with strong shock interactions between the ejecta and any pre-existing circumstellar material, e.g. GK Per (Shara et al. 2012) and T Pyx (Shara et al. 1989), do not fit this relationship.

To estimate how bright the shells around NLs might be, we used as a guide the archetypal old nova DQ Her (Nova Her 1934) which has a clearly visible shell (Slavin et al. 1995). Its shell had a brightness of 1.01×10^{-15} ergs/s/cm^2/arcsec^2 and a radius of $8''$ in May 1982, 47.5 years after its nova eruption (Ferland et al. 1984). This implies that 100 years after outburst it will fade to 2.44×10^{-17} ergs/s/cm^2/arcsec^2, by which time its radius will have doubled to $16''$, and at 200 years after outburst it will fade to 7.63×10^{-19} ergs/s/cm^2/arcsec^2, and its radius will have doubled again to $32''$. We can use these estimates to determine our observing strategy and to establish the instrumental setup that is required.

Nova-like variables have apparent magnitudes of ∼15, on average. Novae brighten by ∼10 magnitudes during eruption, implying that most nova-like variables when in outburst would have been just visible to the naked eye. Given the much increased rate of nova detection in the last 100 years, it is very unlikely that such eruptions would have been missed if they had occurred within the last ∼100 years or so. We thus expect to have to detect shells around nova-like variables which are at least 100 years old; any which

erupted more recently than this would likely have been detected and would now be classified as a nova. Assuming the shell of DQ Her is representative, a 100-year old shell would be at least 16″ in radius and no brighter than 2.44×10^{-17} ergs/s/cm^2/arcsec^2. Hence to detect such shells we require deep images with a relatively modest field of view, which led us to use the Auxiliary Port on the 4.2m William Herschel Telescope (WHT) on La Palma (see Sec. 2.1.2).

To estimate the age of the faintest shell we might detect with this setup, we simulated the images we would obtain from a spherical nova shell in an 1800 second Hα-exposure. The simulation showed that a shell with luminosity comparable to the shell of DQ Her would become too faint to detect in an image at $\sim$ 180 years after outburst. For approximately circular, small shells that are centred on the binary, this detection threshold can be pushed fainter by computing the mean radial profile of the central object and inspecting the wings for evidence of a shell (see Gill & O'Brien 1998). The DQ Her shell would be apparent in the radial profile up to 220 years after outburst. Assuming DQ Her is representative, this means that we would be able to detect shells around nova-like variables from nova eruptions up to a maximum of $\sim$220 years ago using our proposed setup on the WHT.

2.1.2 Observations

The observations were taken on the nights of 1997 October 24–26. We used the 1024×1024 pixels TEK5 CCD chip mounted on the Auxiliary Port[1] at the Cassegrain focus of the WHT to image the fields around our target nova-like variables. This setup gave a platescale of 0.11″ per pixel and hence a field size of 113″ × 113″. Hα is one of the strongest features in the spectra of nova shells, with typical velocity widths of up to 2000 km s^{-1} (e.g. Warner 1995). In order to maximise the detection of light from the shell and minimise the contribution of sky, we therefore used a narrow-band (55Å FWHM = 2500 km s^{-1}) interference filter centred on the rest wavelength of Hα (ING filter number 61[2]). Note that this filter also includes a contribution from [NII] 6584Å emission, which may dominate the spectra of nova shells with strong shock interaction of the ejecta with any pre-existing circumstellar medium, e.g. T Pyx (Shara et al. 1989).

As we were planning to compare the radial profiles of the target stars with field stars, we had to ensure that we did not saturate the target stars. Hence the CCD chip was used unbinned and in quick readout mode, in order to decrease dead-time, at the expense of a negligible decrease in signal-to-noise (thanks to the fact that our observations were always sky-limited). The observing conditions were excellent throughout the run; the sky was always photometric, there was no evidence of dust and the seeing was usually subarcsecond, with an occasional excursion up to 1.5–2″.

2.1.3 Target selection

To ensure we only targeted relatively well-studied systems with reliable CV classifications, we made our selection from the catalogue of Ritter & Kolb (2003)[3] (hereafter RK catalogue). We selected a total of 31 CVs, predominantly NLs, and searched for nova shells around them. To test our setup we included three systems with known nova shells, BT Mon, DQ Her and GK Per. We also took the opportunity to observe two asynchronous polars, which are CVs with magnetic WDs in which the spin period of the WD is not synchronised with the orbital period (Warner 1983). The asynchronicity is believed to be due to a recent nova event, as shown by the system V1500 Cyg which had a nova eruption in 1975 (Stockman et al. 1988). The two asynchronous polars we observed with the WHT were V1432 Aql and BY Cam. We also included three other non-NL systems, PQ Gem, which is an intermediate polar, IP Peg which is a DN, and AY Psc which is a Z Cam-type DN, which were favourably positioned during our observing run.

A full list of the 31 objects observed with the WHT and a journal of observations is given in Tab. 1. In summary, the targets comprised 3 old novae with known shells, 1 old nova without a known shell (V Per), 2 asynchronous polars, 1 intermediate polar, 22 NLs, and 2 DNe. In Fig. 1 we show the orbital period distribution of all the systems we observed with the WHT compared to the total number of systems in the RK catalogue. We deliberately selected a substantial number of the systems in the 3–4 hr orbital period range, which is where most NLs appear, as shown in Fig. 18 of Knigge et al. (2011).

2.1.4 Data reduction

The images were debiased using the median level of the overscan strip and flat-fielded using normalised twilight sky flats. Where we had taken multiple images of targets, these were combined to improve the signal-to-noise ratio. Sky subtraction was performed by subtracting the median level determined from two blank sky areas of size 100 × 100 pixels. Each frame suffered from significant vignetting in the corners due to the circular filter holder, which was not fully corrected by the flat field. The corners of each image were hence removed by setting a series of 50 × 50 pixel blocks to a fixed value, so that they appear white in the final images shown in Appendix A. Pixels affected by cosmic rays were set to the average value of surrounding pixels. All processing was performed using the KAPPA and FIGARO packages in the STARLINK[4] suite of programs.

2.2 Isaac Newton Telescope

2.2.1 Observations

In support of our WHT observations, we also examined known CVs in the 2.5m Isaac Newton Telescope (INT) Photometric Hα Survey of the Northern Galactic Plane (IPHAS). IPHAS is a 1800 deg^2 survey of the northern Milky Way spanning the galactic latitude range $-5^\circ < b < +5^\circ$

[1] http://www.ing.iac.es/astronomy/observing/manuals/html_manuals/wht_instr/pfip/prime3_www.html
[2] http://catserver.ing.iac.es/filter/
[3] http://www.mpa-garching.mpg.de/RKcat/
[4] http://starlink.jach.hawaii.edu/starlink

Table 1. Journal of WHT observations. The classifications of the CVs have been taken from the RK catalogue. The date refers to the start time of the first exposure. All shells detected in our WHT observations are shown in bold and discussed in Sect. 3.1. Note that the RK catalogue classifications for novae are N, Na, Nb. *We detected a shell around V1315 Aql with the INT, not the WHT – see section 3.2.5. †This system is a NL.

Object	Classification	Orbital period (hrs)	Date	UTC start	UTC end	Number of exposures	Total exposure time (secs)	Visible shell?
PX And	NL SW NS SH	3.51	25/10/97	00:06	01:11	2	3600	N
UU Aqr	NL UX SW SH	3.93	25/10/97	22:42	23:46	3	3300	N
HL Aqr	NL UX SW	3.25	27/10/97	00:13	00:54	2	2400	N
V794 Aql	NL VY	3.68	26/10/97	21:17	21:58	2	2400	N
V1315 Aql	NL UX SW	3.35	26/10/97	19:32	20:15	4	2400	N*
V1432 Aql	NL AM AS	3.37	25/10/97	19:59	21:01	2	3600	N
WX Ari	NL UX SW	3.34	25/10/97	02:42	03:44	2	3600	N
KR Aur	NL VY NS	3.91	26/10/97	03:50	04:10	1	1200	N
V363 Aur	NL UX SW	7.71	25/10/97	05:09	06:10	2	3600	N
BY Cam	NL AM AS	3.36	25/10/97	04:00	05:01	2	3600	N
AC Cnc	NL UX SW	7.21	27/10/97	03:31	04:12	2	2400	N
V425 Cas	NL VY	3.59	24/10/97	22:29	22:37	2	200	N
V751 Cyg	†VY SW? NS SS	3.47	24/10/97	22:07	22:27	1	1200	N
V1776 Cyg	NL UX SW	3.95	25/10/97	21:31	22:32	2	3600	N
CM Del	NL UX VY?	3.89	26/10/97	20:22	21:05	4	2400	N
PQ Gem	NL IP	5.19	27/10/97	02:41	03:22	2	2400	N
DQ Her	**Na DQ**	**4.65**	**25/10/97**	**19:31**	**19:51**	**1**	**1200**	**Y**
BH Lyn	NL SW SH NS	3.74	26/10/97	04:24	05:05	2	2400	N
BP Lyn	NL UX SW	3.67	27/10/97	04:21	05:02	2	2400	N
BT Mon	**Na SW**	**8.01**	**26/10/97**	**06:12**	**06:43**	**2**	**1800**	**Y**
BT Mon	**Na SW**	**8.01**	**27/10/97**	**06:02**	**06:32**	**1**	**1800**	**Y**
V1193 Ori	NL UX SW?	3.96	26/10/97	01:05	02:38	3	5400	N
IP Peg	DN UG	3.80	25/10/97	21:08	21:19	1	621	N
LQ Peg	NL VY SH NS	3.22	26/10/97	22:37	23:18	2	2400	N
V Per	Na NL SW?	2.57	27/10/97	01:06	01:48	2	2400	N
GK Per	**Na DN IP**	**47.92**	**25/10/97**	**06:14**	**06:34**	**1**	**1200**	**Y**
AY Psc	DN ZC NS	5.21	25/10/97	23:51	00:53	2	3600	N
VY Scl	NL VY	3.98	24/10/97	23:22	00:03	2	2400	N
VZ Scl	NL VY SW	3.47	24/10/97	22:47	23:39	2	3000	N
SW Sex	NL UX SW	3.24	26/10/97	05:15	05:56	2	2400	N
RW Tri	NL UX SW	5.57	25/10/97	01:29	02:30	2	3600	N
DW UMa	NL SW SH NS	3.28	27/10/97	05:09	05:50	2	2400	N

and galactic longitude range $29^\circ < l < 215^\circ$. Three filters were used, Hα, Sloan r' and Sloan i', reaching down to $r' \approx 20$ (10σ). The survey took place between 2003 and 2008. The survey used the INT Wide Field Camera (WFC) which offers a pixel scale of $0.33''$ per pixel and a field of view of $\sim 34' \times 34'$. Exposure times were initially set at 120 s (Hα) and 10 s (r' and i') but evaluation of the early data led to an increase in the r'–band exposure time to 30 s – for full details of the observations and data reduction see Drew et al. (2005) and Barentsen et al. (2014).

2.2.2 Target selection

We cross-matched the RK catalogue to the IPHAS footprint. There were 74 matches of CVs with the classification N, NL or DN (indicating nova, nova-like variable and dwarf nova, respectively). Each matching IPHAS field was reviewed visually to determine whether any nebulosity was apparent around the target CVs. Due to the significant Hα nebulosity in the Galactic plane, we did not attempt to compute radial profiles for the IPHAS targets.

The 74 systems we examined in IPHAS are listed in Tab. 2. The targets comprised 2 asynchronous polars, 10 polars & intermediate polars, 5 NLs, 34 DNe, 3 old novae with known shells and 20 old novae without known shells. Three of the NLs, V1315 Aql, V363 Aur and V751 Cyg, were also part of our WHT sample, as was BT Mon, an old nova with a known shell.

3 RESULTS

3.1 WHT Images and Radial Profiles

In order to detect shells in the WHT images, we adopted two strategies. First, we visually examined each image to determine if a shell is visible. This technique would reveal wide shells with diameters of more than a few arcseconds. Second, we calculated the radial profile of each CV and compared it to a number of field stars in the same image. Any

Table 2. List of CVs examined in the IPHAS database. The classifications of the CVs have been taken from the RK catalogue. Note that the RK catalogue classifications for novae are N, Na, Nb. All shells detected in IPHAS are shown in bold and are discussed in Sect. 3.2. *We confirmed the detection of a shell around V1315 Aql with additional INT observations – see section 3.2.5. †This system is a NL. ‡Whilst these objects are shown as possible Z Cam systems in the RK catalogue, Simonsen et al. (2014) found that they do not exhibit the standstills necessary for this classification and that they are actually normal DNe.

Object	Classification	Orbital period (hrs)	Visible shell?	Object	Classification	Orbital period (hrs)	Visible shell?
CI Aql	Nr	14.83	N	V2468 Cyg	Na	3.49	N
KX Aql	DN SU	1.45	N	V2491 Cyg	Na	2.56	N
V368 Aql	Na	16.57	N	V446 Her	Na DN	4.97	N
V603 Aql	Na SH NS	3.32	N	CP Lac	Na SW?	3.48	N
V1315 Aql	**NL UX SW**	**3.35**	**Y***	DI Lac	Na	13.05	N
V1425 Aql	Na NL? IP?	6.14	N	**BT Mon**	**Na SW**	**8.01**	**Y**
V1493 Aql	Na	3.74	N	CW Mon	DN UP IP?	4.24	N
V1494 Aql	Na	3.23	N	V902 Mon	NL IP	8.16	N
FS Aur	DN UG IP PW?	1.43	N	V959 Mon	N	7.10	N
HV Aur	DN SU	1.98	N	CZ Ori	DN UG	5.25	N
T Aur	**Nb**	**4.91**	**Y**	V344 Ori	DN ZC‡	5.62	N
QZ Aur	Na	8.58	N	FO Per	DN UG? ZC?‡	4.13	N
V363 Aur	NL UX SW	7.71	N	FY Per	NL VY	6.20	N
AF Cam	DN UG	7.78	N	TZ Per	DN ZC	6.31	N
FT Cam	DN SU?	1.80	N	UV Per	DN SU	1.56	N
V705 Cas	Na	5.47	N	V Per	N NL SW?	2.57	N
V709 Cas	NL IP	5.33	N	WY Sge	N DN? SW?	3.69	N
V1033 Cas	NL IP	4.03	N	DO Vul	DN SU	1.38	N
HT Cas	DN SU	1.77	N	QQ Vul	NL AM	3.71	N
KP Cas	DN SU	1.95	N	V405 Vul	DN SU	2.71	N
EM Cyg	DN ZC	6.98	N	**V458 Vul**	**Na**	**1.64**	**Y**
EY Cyg	DN UG SH?	1.10	N	V498 Vul	DN SU WZ	1.41	N
V337 Cyg	DN SU	1.64	N	GD 552	DN? WZ?	1.71	N
V503 Cyg	DN SU NS	1.87	N	Lanning 420	DN SU	1.45	N
V516 Cyg	DN UG	4.11	N	J0130+6221	DN?	3.12	N
V550 Cyg	DN SU	1.62	N	J0345+5335	CV DN?	7.53	N
V751 Cyg	†VY SW? NS SS	3.47	N	J0506+3547	DN SU	1.62	N
V1251 Cyg	DN SU WZ	1.77	N	J0518+2941	NL?	5.72	N
V1316 Cyg	DN SU	1.78	N	J0524+4244	NL AM AS	2.62	N
V1363 Cyg	**DN ZC?‡**	**2.42**	**Y**?	J0619+1926	DN SU WZ	1.34	N
V1454 Cyg	DN SU	1.36	N	J1853-0128	NL IP	n/a	N
V1500 Cyg	**Na NL AM AS**	**3.35**	**Y**	J1915+0719	DN SU WZ	1.37	N
V2274 Cyg	Na	7.20	N	J1926+1322	NL IP	4.58	N
V2275 Cyg	**Na IP?**	**7.55**	**Y**?	J1953+1859	DN SU?	1.44	N
V2306 Cyg	NL IP	4.35	N	J2133+5107	NL IP	7.14	N
V2362 Cyg	Na	1.58	N	J2138+5544	NL IP	n/a	N
V2467 Cyg	Na NL IP?	3.83	N	J2250+5731	NL AM	2.90	N

nebulosity around the CV due to a nova shell would cause the radial profile of the CV to lie above the average profile of the field stars (for example, see the radial profile of BT Mon in Fig. A4). This technique can reveal shells with diameters of less than a few arcseconds, and was successfully used by Gill & O'Brien (1998) to discover four new nova shells. A key assumption in this technique is that the Point Spread Function (PSF) is uniform across the WHT chip. Fig. 2 shows the PSFs for five field stars (arrowed) in the image of V Per. The PSFs show identical radial profiles irrespective of field position, giving confidence that the PSFs are uniform across the field of view of the CCD, as expected.

The centroids of the stars were first measured by fitting a two-dimensional Gaussian. The radial profiles were then generated by calculating the radial distance of each pixel from the centroid, and then averaging the fluxes of the pixels falling into bins of increasing radial distance from the centroid. The radial profiles were then normalised to unity, and plotted from the centre of the star until the flux reached 1σ above the mean background flux.

In Appendix A we show the images and radial profiles for all of the objects that were observed with the WHT. As expected, the images for the three old novae with previously known shells (BT Mon, DQ Her, GK Per) clearly show a shell and each is discussed briefly below. There are no visible shells in the images of the remaining objects, nor do any of the radial profiles differ significantly from the field stars.

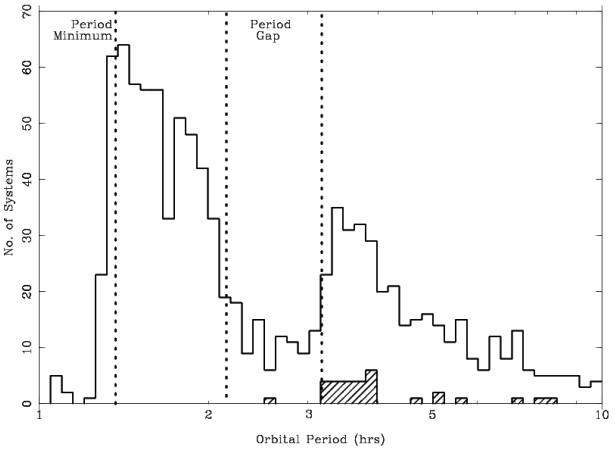

Figure 1. Orbital period distribution of the systems we observed with the WHT (hatched) compared to the distribution of all the CVs in the RK catalogue. The left-hand dotted line indicates the period minimum and the central and right-hand dotted lines show the period gap taken from Knigge et al. (2011).

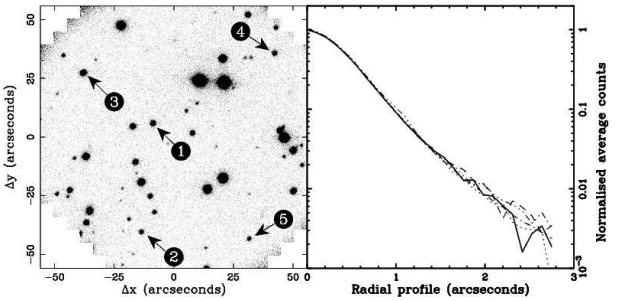

Figure 2. Left: WHT image of V Per (Star number 1). Right: PSFs for the five arrowed stars showing the uniformity across the WHT chip. Each numbered star has been plotted as follows 1 - solid line, 2 - dashed, 3 - dot-dashed-dot-dashed, 4 - dotted, 5 - dashed-dot-dot-dot-dashed. The orientation of the image is the same as that shown in Fig. 3.

3.1.1 BT Mon

The shell around BT Mon (Nova Mon 1939) was discovered spectroscopically by Marsh et al. (1983). BT Mon is a high-inclination system and the system parameters were derived by Smith et al. (1998). The first image of the shell was reported by Duerbeck (1987), who found it to be an incomplete clumpy, slightly elliptical ring with approximate dimensions of $11'' \times 9''$ and the major axis pointing in the NW–SE direction.

Our image and radial profile of BT Mon is shown in Fig. A4. The lower right quadrant was not used to calculate the radial profile in order to remove the flux from the nearby star. The radial profile of BT Mon clearly deviates from the profile of the field stars, from approximately $4''$ outwards. This is due to the presence of the shell and gives assurance that our technique for identifying shells is valid.

In Fig. 3 we show an enlarged version of our image of the BT Mon shell. We estimate the shell diameter to be $13'' \pm 1''$. Assuming a constant shell expansion velocity of 1800 ± 300 km s^{-1} and a distance of 1.8 ± 0.1 kpc as derived

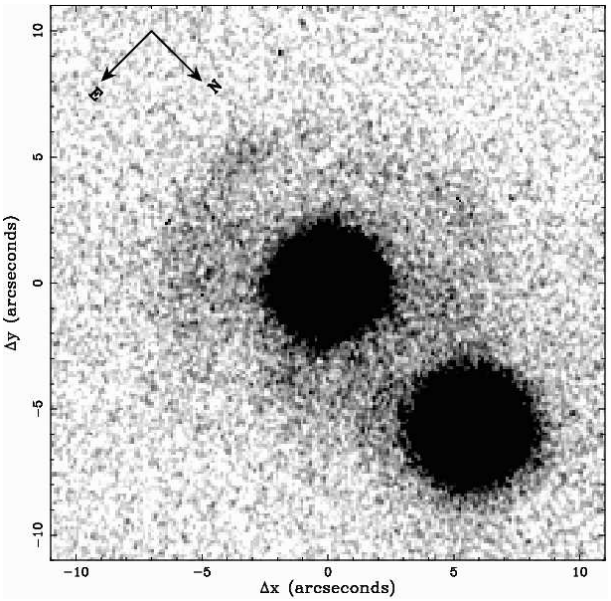

Figure 3. Enlarged image of the BT Mon nova shell. Note that the second star to the lower right is an unassociated foreground/background star.

by Marsh et al. (1983), together with the date of the nova as 1939.7, gives an expected diameter of $12 \pm 3''$ at the time of our observations, in agreement with our measured value.

3.1.2 DQ Her

DQ Her (Nova 1934) is an intermediate polar with system parameters derived by Horne et al. (1993). The nova shell (see Fig. A4) is a prolate ellipsoid with a slightly pinched central ring. Vaytet et al. (2007) used our WHT image of DQ Her to estimate the angular size and hence distance of the system. They measured the angular size of the major and minor axes to be $a = 25.31 \pm 0.44''$ and $b = 18.70 \pm 0.44''$. Assuming a constant expansion velocity of 370 ± 14 km s^{-1}, they derived a distance of $d = 525 \pm 28$ pc.

3.1.3 GK Per

The nova GK Per (1901) is the archetypal nova remnant and has been extensively studied (see Shara et al. (2012) for a review). The shell is boxy in shape, of size approximately $100'' \times 90''$ and exhibits clumpy knots (see Fig. A5). Recently, Liimets et al. (2012) derived a three dimensional model of the nova shell in GK Per, and determined the proper motion and radial velocities of more than 200 knots in the ejecta. The knots have a wide range of velocities (600–1000 km s^{-1}) and have suffered only modest deceleration. Shara et al. (2012) used HST images from 1995 and 1997 to resolve over 1000 filamentary structures in the ejecta. They also investigated a jet-like feature, first discovered by Anupama & Prabhu (1993), which they suggest could be the shock interaction of a collimated flow with the ISM, probably originating from the accretion disc. The jet extends some $2.7'$ to the NW, which is larger than the field of view of our image. We examined our image of GK Per but could not

find any evidence of the jet-like feature on smaller spatial scales, most probably due to the lower signal-to-noise ratio of our image.

3.2 IPHAS images

We visually examined the IPHAS images for evidence of nova shells. Tab. 2 lists all of the objects we examined, and indicates whether a shell is visible. The short exposure times of the Hα images (120 s) means that only bright, nearby shells are likely to be visible. We found three old novae with shells that are visible in the IPHAS footprint: T Aur (Nova Aurigae 1891), V458 Vul (Nova Vul 2007 No. 1) and V1500 Cyg (Nova Cygni 1975), all of which are well studied systems. We briefly review these objects below. We found no definite detections of shells around any other IPHAS targets with the exception of two systems, V1363 Cyg and V1315 Aql, as discussed below. We did discover a nebula around V2275 Cyg, which is too large to be associated with its nova event in 2001. This nebula may be a light echo due either to scattering off, or flash ionisation of, a pre-existing nebula. We also discuss this object further below.

3.2.1 T Aur

The IPHAS Hα image of T Aur is shown in Fig. 4a. The shell is clearly discernible in the image giving us confidence that it is possible to see nova shells in the IPHAS images. The shell structure has been likened to that of DQ Her, although T Aur is some 43 years older (Slavin et al. 1995). The shell is elliptical in shape, with major and minor axes of length $\sim 30'' \times 20''$ respectively.

3.2.2 V458 Vul

The Hα image of V458 Vul is shown in Fig. 4b. The shell has major and minor axes of $\approx 30'' \times 20''$. The image was taken in June 2007, two months before the system underwent a nova explosion in August 2007. The shell is actually a pre-existing planetary nebula ejected some 14,000 years ago (Wesson et al. 2008). The central binary is most likely a post-double common-envelope binary comprised of a WD of mass ~ 1.0 M$_\odot$ and a post-AGB secondary of mass ~ 0.6 M$_\odot$ (Rodríguez-Gil et al. 2010).

3.2.3 V1500 Cyg

V1500 Cyg (Nova Cygni 1975) is a well-studied nova and is the archetypal asynchronous polar (Wade et al. 1991). The nova shell was first imaged four years after outburst by Becker & Duerbeck (1980), who measured the radius at $\sim 1.0''$. Subsequently, Wade et al. (1991) presented an image taken in 1987 by which time the shell had expanded to $\sim 1.9''$, giving an expansion rate of $0.16''$ per annum, and Slavin et al. (1995) presented an image taken in 1993 showing a nebular radius of $\sim 3''$. The IPHAS Hα image taken in 2004 is shown in Fig. 4c. The nova shell is extremely faint and has a radius of $\sim 5''$, still consistent with the nebular expansion rate of $\sim 0.16''$ per annum given by Wade et al. (1991).

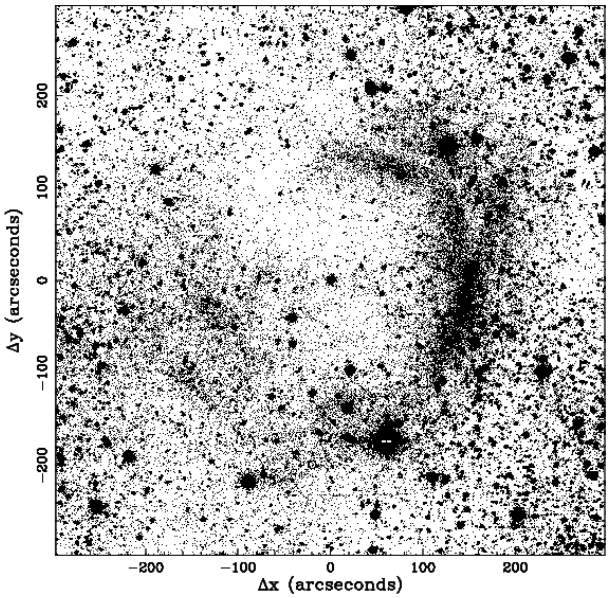

Figure 5. Hα image of the nebula surrounding V1315 Aql. The image is $10' \times 10'$, with North up and East to the left. V1315 Aql is the bright star located at the centre of the image.

3.2.4 V1363 Cyg

In Fig. 4d we show the IPHAS Hα image of the dwarf nova V1363 Cyg. The Hα image is heavily populated with field stars making the surrounding nebula difficult to discern. Hence we show the H$\alpha - r'$ image in Fig. 4e, which effectively removes most of the flux from the field stars. The field is extremely crowded and the object lies close to a ribbon of gas, making the unambiguous detection of a nova shell extremely difficult. However, there is a faint egg-shaped shell of emission of $\approx 2'$ diameter, approximately centred on the CV.

3.2.5 V1315 Aql

Figs. 4f & 4g show the IPHAS Hα and H$\alpha - r'$ images of V1315 Aql. There is a faint shell of $\approx 2.5'$ radius approximately centred on the CV, with more pronounced emission towards the West. We also imaged this object with the WHT. However, the small field of view of our WHT image (see Fig. A1) is not large enough to confirm the possible detection of this shell.

In order to confirm the detection of the shell around V1315 Aql, we took a further 13 exposures of V1315 Aql on 2014 August 2 with the WFC on the INT with a total exposure time of 7200 s in Hα. The stacked Hα image is shown in Fig. 5. The image clearly shows a shell surrounding the central system, with a radius of $\sim 3'$, confirming the proposed detection in Fig. 4. Assuming a shell expansion rate of 2000 km s^{-1} and a distance of 356^{+65}_{-80} pc (Ak et al. 2007), this means that V1315 Aql experienced a nova eruption ~ 120 years ago.

We examined the historic records of nova sightings compiled by Ho (1962) and Stephenson (1976), but found nothing that coincides with the position of V1315 Aql.

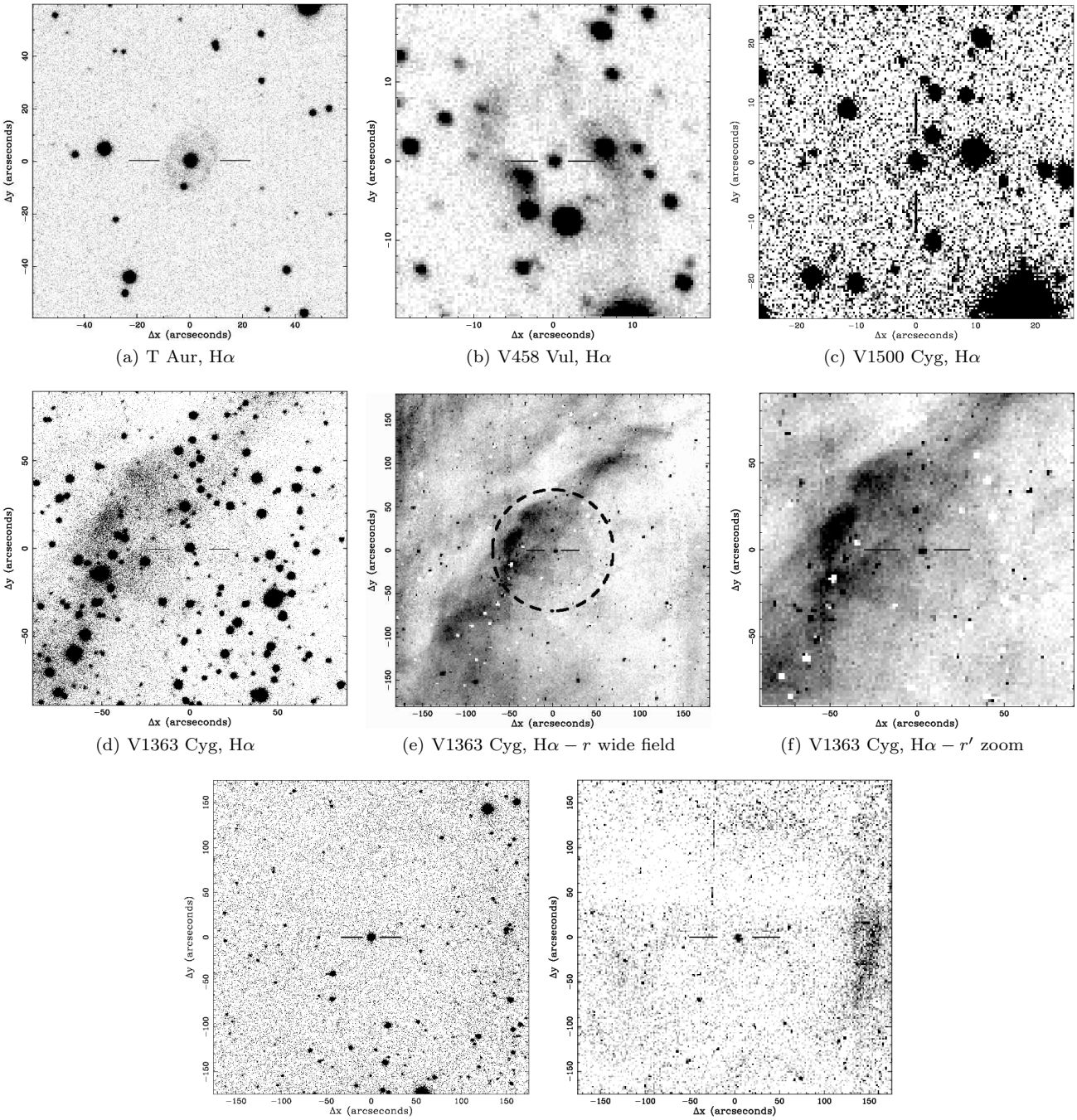

(a) T Aur, Hα (b) V458 Vul, Hα (c) V1500 Cyg, Hα

(d) V1363 Cyg, Hα (e) V1363 Cyg, H$\alpha - r$ wide field (f) V1363 Cyg, H$\alpha - r'$ zoom

(g) V1315 Aql, Hα (h) V1315 Aql, H$\alpha - r'$

Figure 4. IPHAS Hα and H$\alpha - r'$ images. In all images, North is up, East is left.

3.2.6 V2275 Cyg

The nova eruption of V2275 Cyg (Nova Cygni 2001 No. 2) occurred on 2001 August 19 (Nakamura et al. 2001). The field around V2275 Cyg was observed on five epochs during the IPHAS survey. The five images are shown in Figure 6.

In the first three images, taken between November 2003 and November 2006, a nebula of $\approx 2.7'$ diameter is clearly apparent, but it has disappeared in the fourth and fifth images taken in December 2008 and August 2009. Using the expansion velocity and minimum distance derived by Kiss et al. (2002) of approximately 2000 km s^{-1} and 3 kpc respectively, the shell from the 2001 nova event should have been no larger than $0.2'$ by November 2006, which is the date of the last IPHAS image the nebula was visible in. Hence the nebula in the image can not be from the 2001 nova event. The most obvious explanation is that it is a light echo from material ejected from the system by a previous event, such as a nova shell or a planetary nebula. The angular diameter of the shell is $2.7' \pm 0.5'$. Adopting the distance of 3–8 kpc derived by Kiss et al. (2002) using maximum magnitude

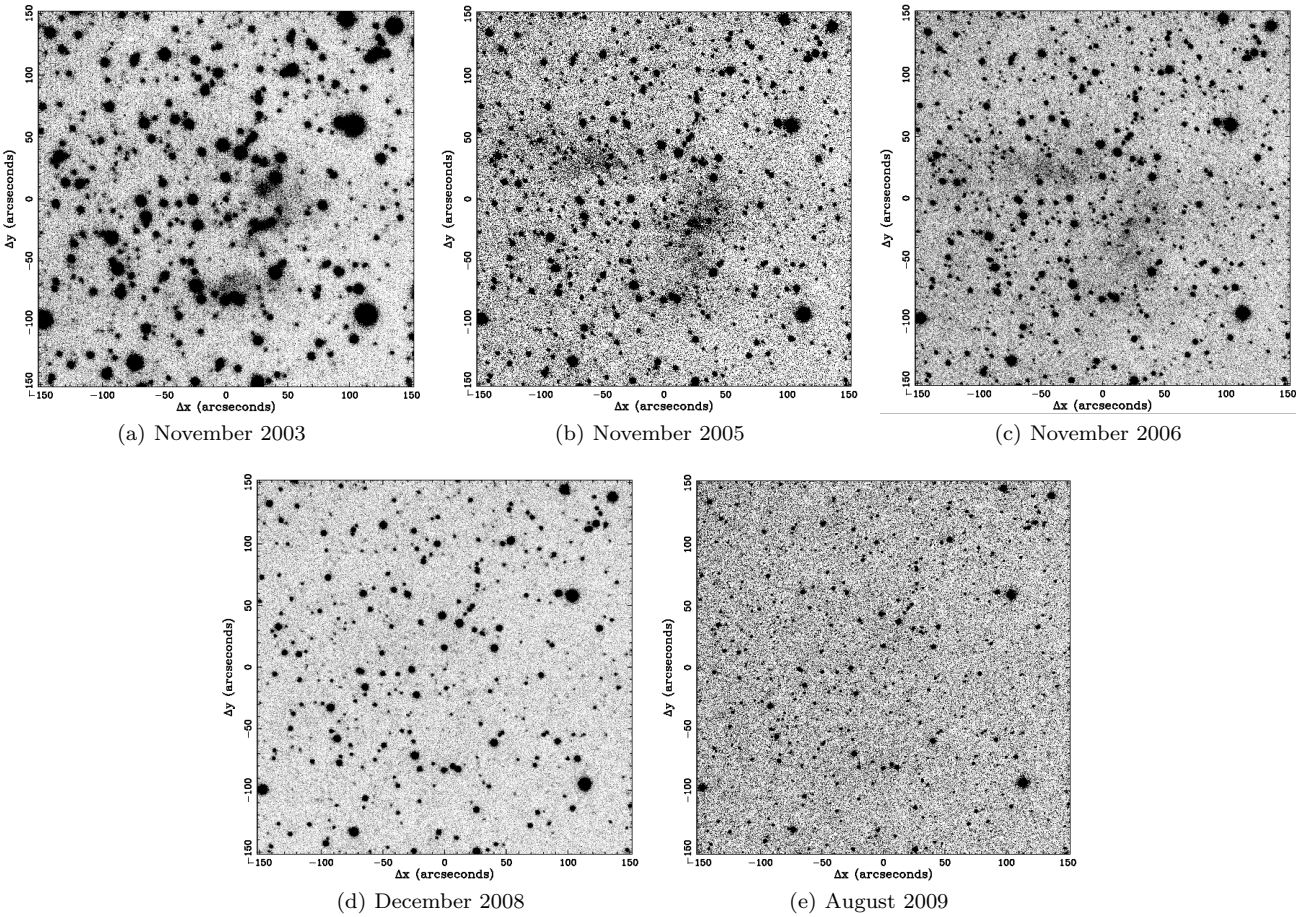

(a) November 2003 (b) November 2005 (c) November 2006

(d) December 2008 (e) August 2009

Figure 6. Hα images of V2275 Cyg from IPHAS. A faint nebula is apparent in images (a)–(c) but is not present in images (d) and (e). In all images, North is up, East is left.

versus rate of decline relationships, the radius of the shell is 3–12 $\times 10^{16}$m. The time from the nova in 2001 to the date of the first IPHAS image is 819 days giving a light radius of 2.1×10^{16}m. These two radii are broadly comparable, as expected for a light echo. Assuming a typical nova shell expansion velocity of 2000 km s^{-1}, the age of the shell can be estimated to be $\sim$ 300 years. We have reviewed the literature and can find no previous discussion of a nebula around V2275 Cyg. Indeed, the presence of light echoes around novae are relatively rare, and only GK Per, V732 Sgr, V458 Vul and T Pyx have recorded echoes (Kapteyn 1901, Swope 1940, Wesson et al. 2008, Sokoloski et al. 2013, respectively).

There are three principal blobs of material that are apparent in the images, as highlighted in Figs 7 a–c. Blob A does not appear in Fig. 7(a) but appears in Figs. 7(b) & 7(c). It appears to move southwards (towards the right in the images) by approximately 20″. At a distance of 3 kpc, with an interval of approximately one year between the two images, this equates to a transverse speed of 2.7×10^8 ms^{-1}. Clearly this cannot be bulk motion of material. It is better explained as the passage of a light pulse through a pre-existing bi-polar nebula, with the axis of symmetry of the nebula pointing approximately perpendicular to the plane of the sky. This orientation is suggested by the lack of eclipses in the light curve of V2275 Cyg (Balman et al. 2005). Blob B appears in all three images and whilst different parts change intensity, there is no consistent motion shown. This blob of material is diagonally opposite blob A and could be the opposite pole of a bi-polar nebula. Blob C only appears in Fig 7(a).

If the shell is due to a previous nova event this would mean that V2275 Cyg should be reclassified as a recurrent nova (RN), in agreement with Pagnotta & Schaefer (2014) who identified V2275 Cyg as a likely RN on the basis of its outburst light curve and spectrum.

4 DISCUSSION

Our goal was to search for previously undetected nova shells around CVs, primarily nova-like variables. The results of our search are shown in Tab. 3.

4.1 Nova-like variables

We surveyed 22 NLs with the WHT and 5 NLs with IPHAS (three NLs were surveyed in both giving a total of 24 unique NLs), and found no shells with the WHT and evidence for only one shell in IPHAS, V1315 Aql, which we subsequently confirmed with additional INT observations (see Sect. 3.2.5).

What can we deduce from our discovery of a shell around one NL? Let us assume that all novae that occurred

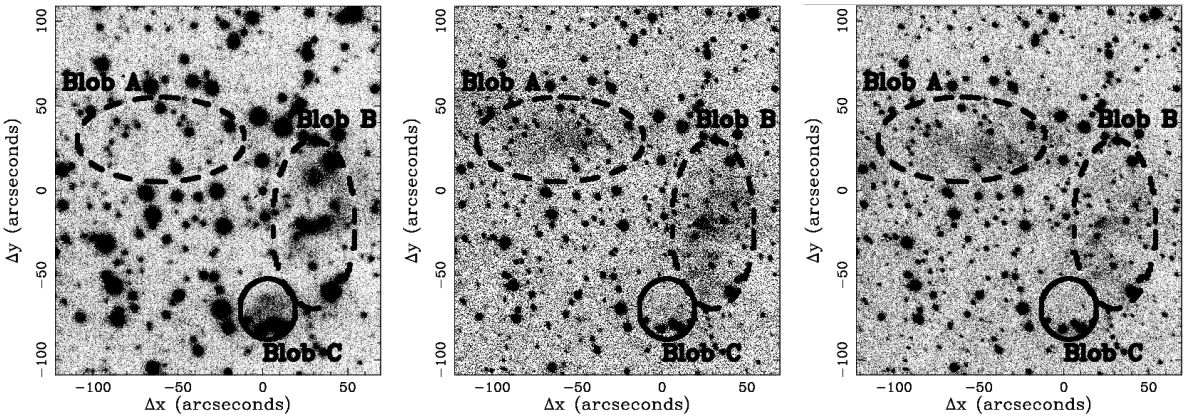

(a) November 2003 (b) November 2005 (c) November 2006

Figure 7. Hα images of V2275 Cyg from IPHAS. See text for a discussion about the three blobs of material. In all images, North is up, East is left.

Table 3. Summary of our search for nova shells.

	Nova-like Variables	Polars & Intermediate Polars	Asynchronous Polars	Dwarf Novae	Old Novae	Total
WHT Targets	22	1	2	2	4	31
IPHAS Targets	5	10	2	34	23	74
less: Duplicated objects	–3	0	0	0	–1	–4
Grand total of systems	24	11	4	36	26	101

in the last $\sim$ 100 years would have been observed. These would now be classified as old novae in the RK catalogue and hence would not appear in our sample of NLs. We also know that our observations are not sensitive to shells older than $\sim$ 200 yrs (see Sect. 2.1.1). Hence our search for nova shells around NLs is only likely to find shells between 100 and 200 years old. We found one shell in this 100-year window, out of 24 NLs surveyed, indicating that the lifetime of the NL phase lasts approximately 2400 yrs. This is consistent with the order-of-magnitude estimate of 1,000 years derived by Patterson et al. (2013) for the NL phase for long-period CVs. Hence our results lend some support to the nova-induced cycle theory, although we are dealing with small number statistics; our survey of 24 NLs represents only 31% of the 78 NLs in the RK catalogue. We also acknowledge the incompleteness of our survey due to the small field of view of the WHT images, and the shallow IPHAS images (see Sect. 4.3 for a discussion). We also note that our IPHAS search included 7 novae with previously discovered shells but we only found 4, and searches for shells around known novae tend to recover shells around only half of the targets (Downes & Duerbeck 2000). With all of the assumptions, uncertainties and survey inefficiencies detailed above, our estimate of the NL-phase lifetime should be viewed as a lower limit.

As we were about to submit this paper, a paper appeared by Schmidtobreick et al. (2015), who presented the results of a survey for nova shells around 10 DNe in the 3–4 hr period range with low-$\dot{M}$ and 5 NLs that show low states (VY Scl stars). They found no shells, and used this to set a lower limit of 13 000 years on the nova recurrence time. This is consistent with the lifetime of the NL phase of $\sim$ 2400 yrs that we have derived, as clearly the NL phase should be shorter than the nova recurrence time, although their figure is arguably even more uncertain than ours.

4.2 Asynchronous polars

The WHT survey included two asynchronous polars, V1432 Aql and BY Cam. The images and radial profiles of these two systems are shown in Appendix A2. There are no traces of nebulosity in either the images or the radial profiles of these systems. There are two other asynchronous polars in the IPHAS survey, J0524+4244 and V1500 Cyg, the archetypal asynchronous polar. There is no evidence of a shell around J0524+4244. We did recover the previously known shell around V1500 Cyg, originating from its nova eruption in 1975 (see Sect. 3.2.3).

Our results imply that we are unable to confirm that a recent nova eruption is the cause of the asynchronicity in the white dwarf spin of these systems. However, it is perhaps not surprising that we did not find any new shells given our survey limits and the synchronisation timescale. BY Cam, for example, is estimated to synchronise within $\sim$ 1100 yrs (Campbell & Schwope 1999), an order of magnitude longer than our 100 yr detection window (see Sect. lifetime).

4.3 Future surveys

In hindsight, our decision to use the old nova DQ Her as a guide for our WHT search strategy (Sect. 2.1.1) led us to underestimate the optimal field of view for hunting for nova shells. This is because DQ Her has relatively slow ejecta ($350\,\mathrm{km\,s^{-1}}$; Warner 1995). The angular size of the shell is determined by the time since the nova eruption, the distance to the CV, and the speed of the ejecta, and is given by the following scaling relation:

$$R \sim 20'' \; \frac{t/100\,\mathrm{yr} \times v/1000\,\mathrm{km\,s^{-1}}}{d/\mathrm{kpc}}, \qquad (1)$$

where R is the angular radius of the shell in arcseconds, t is the time elapsed since the nova eruption, v is the shell expansion velocity, and d is the distance to the CV. Hence a recent, distant nova with slow-moving ejecta ($t = 100, v = 500, d = 2$) would have a small shell of radius $\sim 5''$, whereas an older, nearby nova with fast moving ejecta ($t = 200, v = 2000, d = 0.5$) would have expanded to a radius of $\sim 2.7'$. Hence the field of view of the Auxiliary port on the WHT ($\sim 1'$ radius) was too small to detect such large shells. This is borne out by the size of the one shell that we did discover around V1315 Aql, which is $\sim 2.5'$ in radius, and the two shells discovered by Shara et al. (2007; 2012) of radii $1.5'$ (AT Cnc) and $15'$ (Z Cam). Another problem with having such a small field of view is the paucity of field stars for the radial-profile technique (Sect. 3.1).

The IPHAS survey, on the other hand, had more than enough field of view ($\sim 17'$ radius per pointing) to discover nova shells but suffered from very short exposure times (120 s), which we had no control over, and from being constrained to the Galactic plane, making it difficult to pick out nova shells from the Hα nebulosity. A more optimal survey for nova shells would have approximately the same field of view as an IPHAS pointing, avoid the Galactic plane and be of similar depth to our WHT survey.

5 CONCLUSIONS

We have performed an Hα-imaging survey for nova shells around CVs. We imaged 31 CVs with the WHT, and searched the IPHAS fields around 74 CVs.

Our search focused on looking for shells around nova-like variables, as the nova-induced cycle theory suggests that these systems are most likely to have undergone a recent nova eruption. Of the 24 unique NLs we examined we found evidence for only one shell around V1315 Aql, which has a radius of $\sim 2.5'$, indicative of a nova eruption approximately 120 years ago.

The survey included 4 asynchronous polars, 2 observed with the WHT (V1432 Aql and BY Cam) and 2 in IPHAS (J0524+4244 and V1500 Cyg) but we found no shells around any of them, except the previously known shell around V1500 Cyg. Hence we are unable to confirm whether the asynchronicity of the WD spin in these systems is due to a recent nova eruption.

We find no unambiguous detections of nova shells around other classes of CV, but we did find tentative evidence of a faint shell around the dwarf nova V1363 Cyg (see Sect. 3.2.4). We also find evidence for a light echo around the nova V2275 Cyg, which erupted in 2001, indicative of an earlier nova eruption ~ 300 years ago, thus making V2275 Cyg a possible recurrent nova (see Sect. 3.2.6).

ACKNOWLEDGEMENTS

This paper makes use of data obtained as part of the INT Photometric Hα Survey of the Northern Galactic Plane (IPHAS, www.iphas.org) carried out at the INT. The INT and WHT are operated on the island of La Palma by the Isaac Newton Group in the Spanish Observatorio del Roque de los Muchachos of the Instituto de Astrofisica de Canarias. All IPHAS data are processed by the Cambridge Astronomical Survey Unit, at the Institute of Astronomy in Cambridge. The bandmerged DR2 catalogue was assembled at the Centre for Astrophysics Research, University of Hertfordshire, supported by STFC grant ST/J001333/1. We would specificlly like to thank Janet Drew for her help in accessing the IPHAS data and for her comments on the draft paper, and Jonathan Irwin who prepared the mosaic images. We would also like to thank Jeanne Wilson and Joanne Caffrey for their help with the WHT data reduction. We thank the referee, Mike Shara, for his valuable comments on the paper.

VSD, CK & TRM were supported under grants from the Science and Technology Facilities Council (STFC).

REFERENCES

Ak T., Bilir S., Ak S., Retter A., 2007, New Astronomy, 12, 446
Anupama G. C., Prabhu T. P., 1993, MNRAS, 263, 335
Balman Ş., Yılmaz A., Retter A., Saygaç T., Esenoglu H., 2005, MNRAS, 356, 773
Barentsen G., Farnhill H. J., Drew J. E., González-Solares E. A., Greimel R., Irwin M. J., Miszalski B., Ruhland C., Groot P., Mampaso A., Sale S. E., Henden A. A., Aungwerojwit A., Barlow M. J., Carter P. J., Corradi R. L. M., et al., 2014, MNRAS, 444, 3230
Becker H. J., Duerbeck H. W., 1980, PASP, 92, 792
Büning A., Ritter H., 2004, A&A, 423, 281
Campbell C. G., Schwope A. D., 1999, A&A, 343, 136
Downes R. A., Duerbeck H. W., 2000, ApJ, 120, 2007
Downes R. A., Duerbeck H. W., Delahodde C. E., 2001, Journal of Astronomical Data, 7, 6
Drew J. E., Greimel R., Irwin M. J., Aungwerojwit A., Barlow M. J., Corradi R. L. M., Drake J. J., Gänsicke B. T., Groot P., Hales A., Hopewell E. C., Irwin J., Knigge C., Leisy P., Lennon D. J., Mampaso A., Masheder M. R. W. ., et al., 2005, MNRAS, 362, 753
Duerbeck H. W., 1987, The ESO Messenger, 50, 8
Ferland G. J., Williams R. E., Lambert D. L., Slovak M., Gondhalekar P. M., Truran J. W., Shields G. A., 1984, ApJ, 281, 194
Gänsicke B. T., Dillon M., Southworth J., Thorstensen J. R., Rodríguez-Gil P., Aungwerojwit A., Marsh T. R., Szkody P., Barros S. C. C., Casares J., de Martino D., Groot P. J., Hakala P., Kolb U., Littlefair S. P., Martínez-Pais I. G., et al., 2009, MNRAS, 397, 2170
Gill C. D., O'Brien T. J., 1998, MNRAS, 300, 221
Ho P. Y., 1962, Vistas in Astronomy, 5, 127

Horne K., Welsh W. F., Wade R. A., 1993, ApJ, 410, 357
Kapteyn J. C., 1901, Astron. Nachr., 157, 201
Kiss L. L., Gogh N., Vinkó J., Furész G., Csák B., DeBond H., Thomson J. R., Derekas A., 2002, A&A, 384, 982
Knigge C., 2011, ArXiv e-prints, p. 1101.2901
Knigge C., Baraffe I., Patterson J., 2011, ApJS, 194, 28
Liimets T., Corradi R. L. M., Santander-García M., Villaver E., Rodríguez-Gil P., Verro K., Kolka I., 2012, ApJ, 761, 34
Littlefair S. P., Dhillon V. S., Marsh T. R., Gänsicke B. T., Southworth J., Baraffe I., Watson C. A., Copperwheat C., 2008, MNRAS, 388, 1582
Marsh T. R., Oke J. B., Wade R. A., 1983, MNRAS, 205, 33P
Nakamura A., Tago A., Abe H., 2001, IAU Circ., 7686, 2
Osaki Y., 1974, Pub. Astr. Soc. Japan, 26, 429
Pagnotta A., Schaefer B. E., 2014, ApJ, 788, 164
Patterson J., Kemp J., Harvey D. A., Fried R. E., Rea R., Monard B., Cook L. M., Skillman D. R., Vanmunster T., Bolt G., Armstrong E., McCormick J., Krajci T., Jensen L., Gunn J., Butterworth N., Foote J., Bos M., Masi G., Warhurst P., 2005, PASP, 117, 1204
Patterson J., Uthas H., Kemp J., de Miguel E., Krajci T., Foote J., Hambsch F.-J., Campbell T., Roberts G., Cejudo D., Dvorak S., Vanmunster T., Koff R., Skillman D., Harvey D., Martin B., Rock J., Boyd D., Oksanen A., Morelle E., Ulowetz J., Kroes A., Sabo R., Jensen L., 2013, MNRAS, 434, 1902
Ritter H., Kolb U., 2003, A&A, 404, 301, (Update RKCat 7.20, 2013)
Rodríguez-Gil P., Santander-García M., Knigge C., Corradi R. L. M., Gänsicke B. T., Barlow M. J., Drake J. J., Drew J., Miszalski B., Napiwotzki R., Steeghs D., Wesson R., Zijlstra A. A., Jones D., Liimets T., Others 2010, MNRAS, 407, L21
Schmidtobreick L., Shara M., Tappert C., Bayo A., Ederoclite A., 2015, ArXiv e-prints, p. 1502.05230
Shara M. M., Livio M., Moffat A. F. J., Orio M., 1986, ApJ, 311, 163
Shara M. M., Martin C. D., Seibert M., Rich R. M., Salim S., Reitzel D., Schiminovich D., Deliyannis C. P., Sarrazine A. R., Kulkarni S. R., Ofek E. O., Brosch N., Lépine S., Zurek D., De Marco O., Jacoby G., 2007, Nat, 446, 159
Shara M. M., Mizusawa T., Wehinger P., Zurek D., Martin C. D., Neill J. D., Forster K., Seibert M., 2012, ApJ, 758, 121
Shara M. M., Potter M., Williams R. E., Cohen J., 1989, ApJ, 337, 720
Shara M. M., Zurek D., De Marco O., Mizusawa T., Williams R., Livio M., 2012, AJ, 143, 143
Simonsen M., Boyd D., Goff W., Krajci T., Menzies K., Otero S., Padovan S., Poyner G., Roe J., Sabo R., Sjoberg G., Staels B., Stubbings R., Toone J., Wils P., 2014, Journal of the American Association of Variable Star Observers (JAAVSO), 42, 177
Slavin A. J., O'Brien T. J., Dunlop J. S., 1995, MNRAS, 276, 353
Smith D. A., Dhillon V. S., Marsh T. R., 1998, MNRAS, 296, 465
Sokoloski J. L., Crotts A. P. S., Lawrence S., Uthas H., 2013, ApJ, 770, L33
Stephenson F. R., 1976, QJRAS, 17, 121
Stockman H. S., Schmidt G. D., Lamb D. Q., 1988, ApJ, 332, 282
Swope H. H., 1940, Harvard College Observatory Bulletin, 913, 11
Vaytet N. M. H., O'Brien T. J., Rushton A. P., 2007, MNRAS, 380, 175
Wade R. A., Ciardullo R., Jacoby G. H., Sharp N. A., 1991, AJ, 102, 1738
Warner B., 1983, in Livio M., Shaviv G., eds, Cataclysmic Variables and Related Physics IAU Colloquia No. 72. p. 155
Warner B., 1995, Cataclysmic Variable Stars. Cambridge University Press, Cambridge
Wesson R., Barlow M. J., Corradi R. L. M., Drew J. E., Groot P. J., Knigge C., Steeghs D., Gaensicke B. T., Napiwotzki R., Rodriguez-Gil P., Zijlstra A. A., Bode M. F., Drake J. J., Frew D. J., Gonzalez-Solares E. A., et al., 2008, ApJ, 688, L21

APPENDIX A: WHT IMAGES (IN ALPHABETICAL ORDER OF CONSTELLATION)

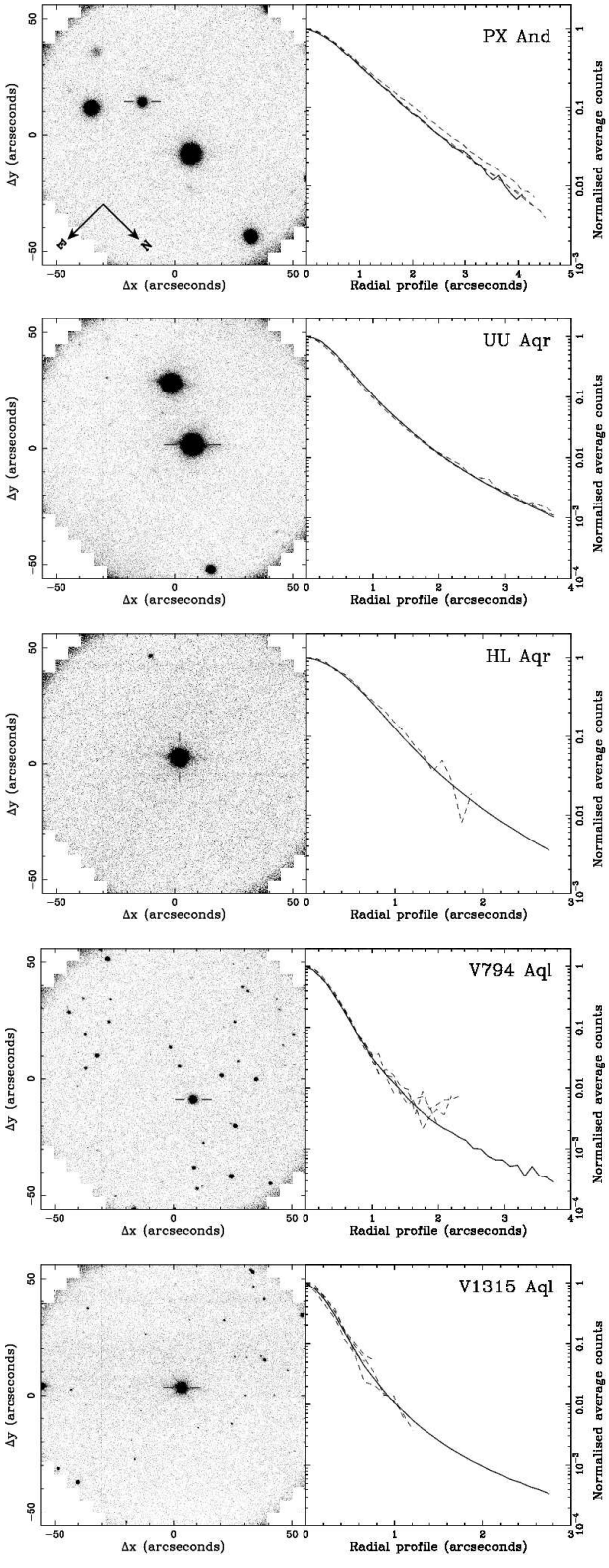

Figure A1. WHT images of our target CVs (left) and the associated radial profiles (right); the solid line is the radial profile of the CV and the dashed lines are field stars. The radial profiles are normalised to unity and plotted until they reach 1σ above the background level. The CVs are marked by bars and are located towards the centres of the images. The orientation of all images is the same, and is shown in the image of PX And.

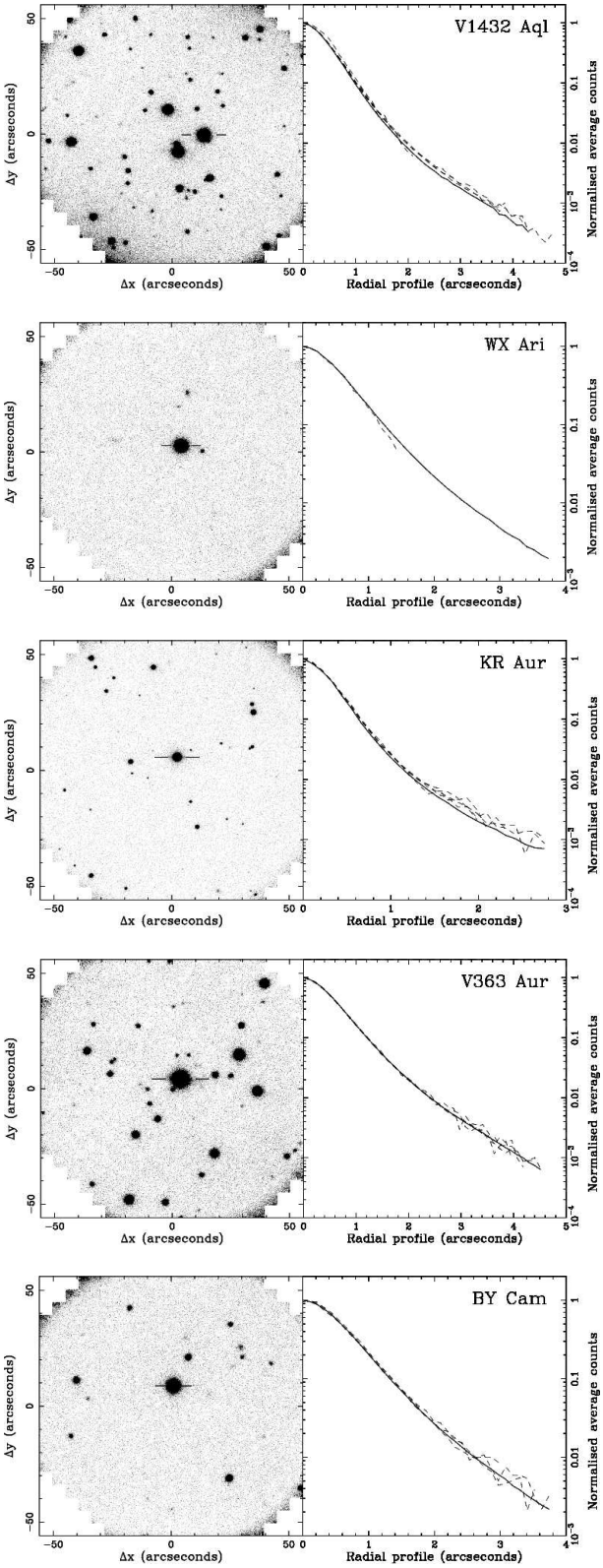

Figure A2. See caption to Figure A1 for details.

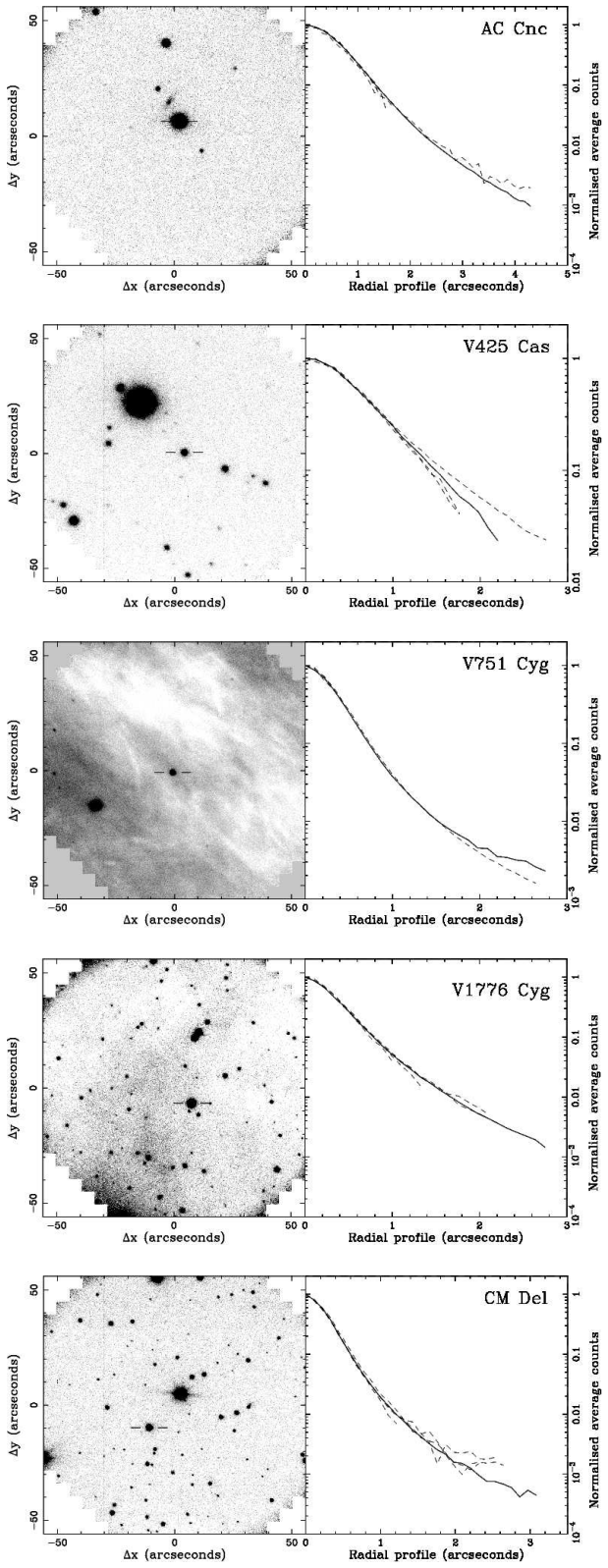

Figure A3. See caption to Figure A1 for details.

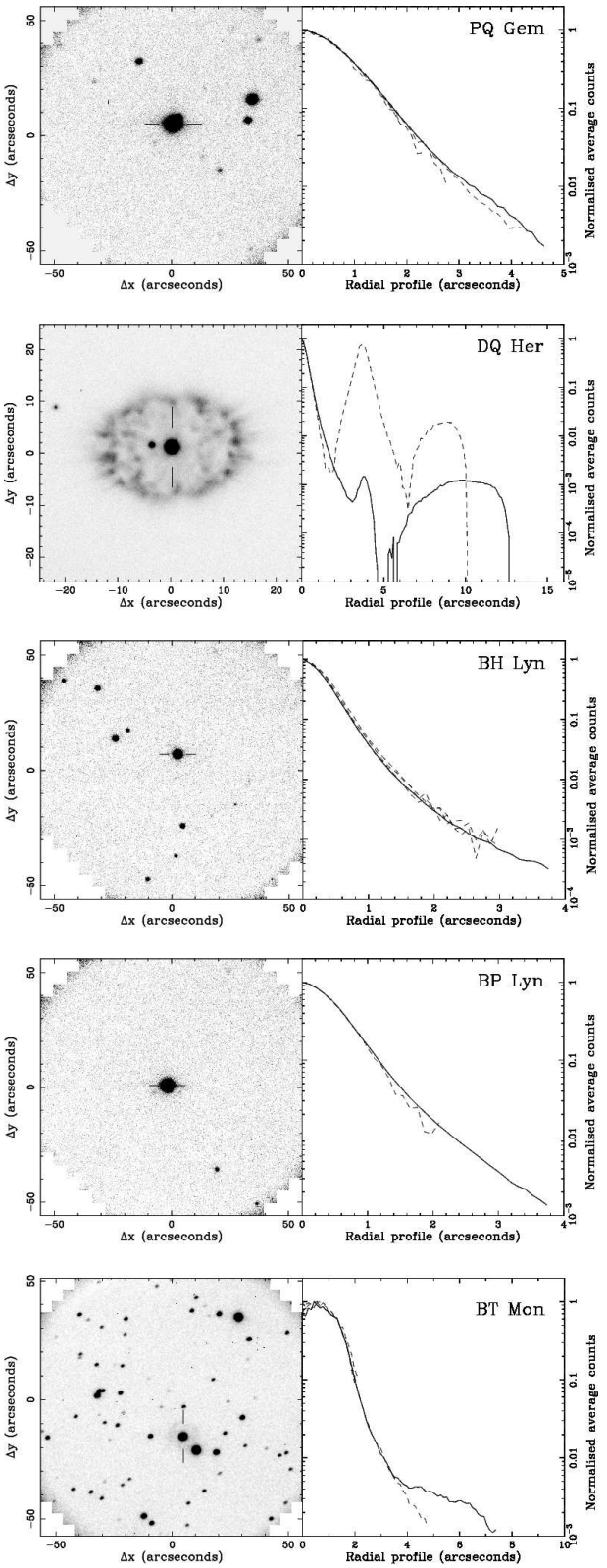

Figure A4. See caption to Figure A1 for details.

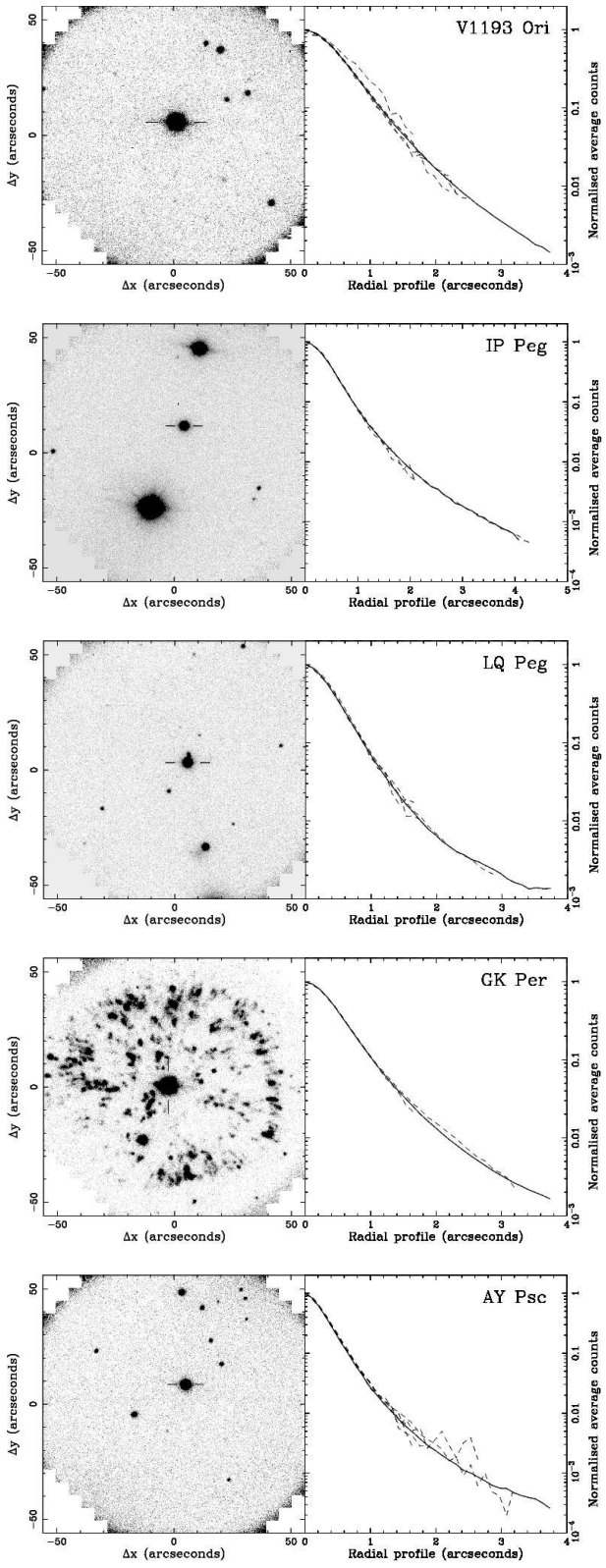

Figure A5. See caption to Figure A1 for details.

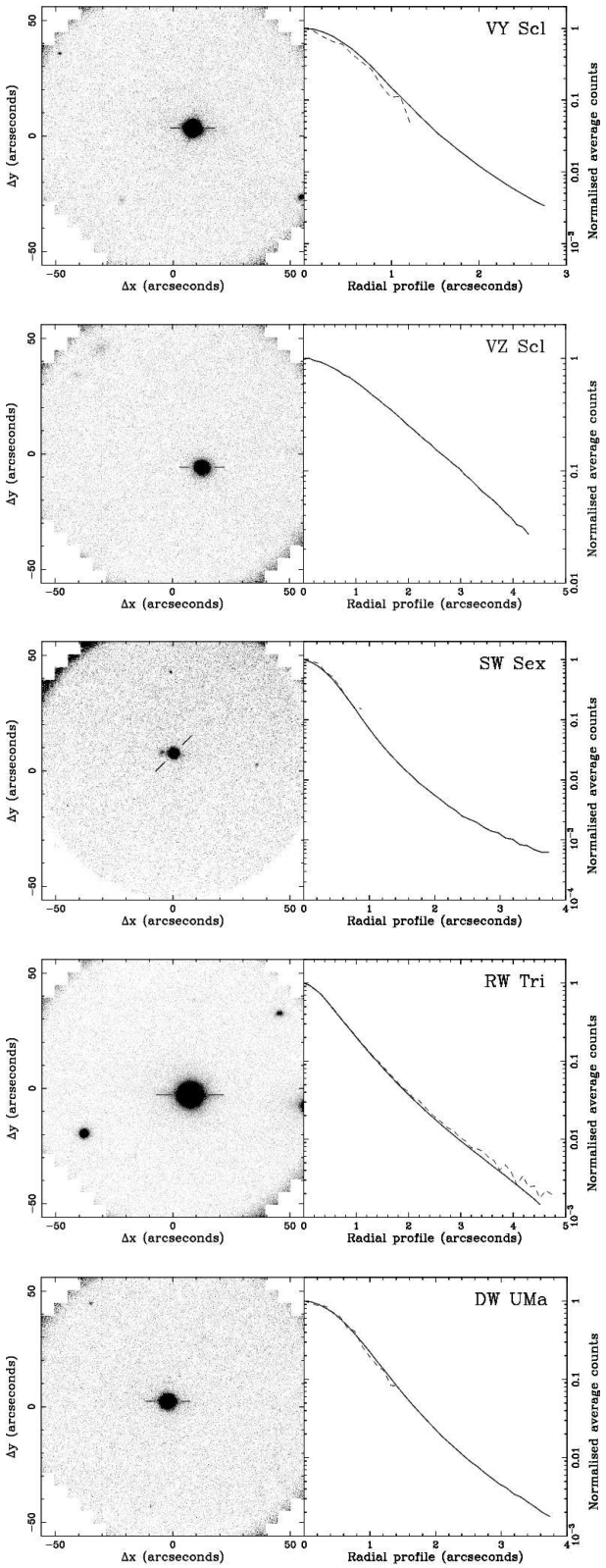

Figure A6. See caption to Figure A1 for details.